

Gigabit/s Optical Receiver Sensitivity and Zero-Dispersion Single-Mode Fiber Transmission at 1.55 μ m

JUN-ICHI YAMADA, AKIO KAWANA, TETSUO MIYA, HARUO NAGAI,
AND TATSUYA KIMURA, SENIOR MEMBER, IEEE

Abstract—High-speed pulse response and receiver sensitivity at 1.55 μ m were measured at data rates ranging from 400 Mbits/s to 2 Gbits/s, in order to elucidate characteristics of a reach-through p^+nn^- Ge APD. The p^+nn^- Ge APD receiver provided a 2 Gbit/s received optical power level of -32.0 dBm at 1.55 μ m and a 10^{-9} error rate, which was 4 dB better than the receiving level with a p^+n Ge APD. Detector performance at 1.3 μ m was also studied for comparison with performance at 1.55 μ m.

Single-mode fibers, which have 0.54 dB/km loss and zero dispersion at 1.55 μ m, and an optical transmitter-receiver, whose repeater gain is 29.2 dB, have enabled 51.5 km fiber transmission at 2 Gbits/s. The transmission system used in this study has a data rate repeater-spacing product of 103 (Gbits/s) \cdot km at 1.55 μ m. Optical pulse broadening and fiber dispersion were also studied, using 1.55 and 1.3 μ m dispersion-free fibers. Future repeater spacing prospects for PCM-IM single-mode fiber transmission systems are discussed based on these experimental results.

I. INTRODUCTION

IN the long wavelength region, single-mode optical fiber transmission systems provide both large transmission capacity and long repeater spacing owing to the low-loss and low-dispersion characteristics of silica fibers [1]. Single-mode fiber transmission technology is expected to play an important role in trunk transmission systems for future telecommunication networks. Conventionally designed single-mode fibers have a relative index difference Δ of around 0.2 percent and a core diameter $2a$ of about 10 μ m. The sum of material and waveguide dispersions approaches zero near 1.3 μ m in single-mode fiber [2]. High-speed optical pulse transmission systems have been realized at the 1.3 μ m wavelength band. A 1.3 μ m optical transmission experiment with a data-rate repeater-spacing product of 88.6 (Gbits/s) \cdot km has already been separately reported by two of the present authors [3]. The 1.3 μ m dispersion-free fibers, however, have an ultimate minimum loss of 0.2 dB/km at 1.55 μ m [4], where the dispersion

amounts to about 20 ps/(km \cdot nm). Optical transmission systems which utilize the 1.55 μ m band will have the longest repeater spacing and largest transmission capacity in silica fiber systems, if a new design makes it possible to remove the transmission bandwidth degradation caused by the dispersion in conventionally designed fibers.

A method to overcome the difficulty in the 1.55 μ m region is to tailor the zero dispersion wavelength to coincide with the minimum loss wavelength [1], [5]. 1.55 μ m dispersion-free fibers have higher Δ s and smaller core diameters than do 1.3 μ m dispersion-free fibers. So, the concern is how low the loss will be in these fibers at 1.55 μ m. An effective alternative is to make directly modulated semiconductor lasers which operate in a single-longitudinal mode. A single frequency optical source has been realized by a distributed feedback laser [6], [7] and a distributed Bragg reflector laser [8], or by using a light injection technique [9] at this wavelength. Otherwise, a dispersion of about 20 ps/(km \cdot nm) in conventionally designed fibers makes it necessary to space repeaters at distances of less than 20 km apart at data rates above 400 Mbits/s [10].

Recently, 1.55 μ m dispersion-free fibers showing a 0.35 dB/km loss have been fabricated [11] by the VAD method, which is also effective for growing fiber preforms continuously [12]. This low loss value indicates a bright potential for 1.55 μ m band transmission.

An optical receiver, with a p^+n Ge avalanche photodiode (APD) [13] used as a photodetector, has worse receiving sensitivity at 1.55 μ m than at 1.3 μ m. Sensitivity degradation at 1.55 μ m is caused by a tailing in optical pulse response, which depends on the diffusion time for carriers generated in an undepleted layer, and poor responsivity due to a decrease in the optical absorption coefficient reduction. Receiver sensitivity at 1.55 μ m can be improved by using a newly developed reach-through type p^+nn^- Ge APD [14], since the reach-through p^+nn^- Ge APD has a longer depleted layer and thinner absorption length than a p^+n Ge APD.

This paper reports an improved 1.55 μ m receiver sensitivity in an optical receiver employing a p^+nn^- Ge APD and 50 Ω Si bipolar transistor front end, for data rates ranging from 400 Mbits/s to 2 Gbits/s. High-speed pulse response in Ge APD's has been studied at various data rates in order to evaluate photodetector performance. Receiver sensitivity and high-speed pulse response in a p^+nn^- Ge APD receiver are compared

Manuscript received February 8, 1982; revised April 14, 1982.

J.-I. Yamada is with the Yokosuka Electrical Communication Laboratory, Nippon Telegraph and Telephone Public Corporation, Yokosuka-shi, Kanagawa, Japan.

A. Kawana, H. Nagai, and T. Kimura are with the Musashino Electrical Communication Laboratory, Nippon Telegraph and Telephone Public Corporation, Musashino-shi, Tokyo, Japan.

T. Miya is with the Ibaraki Electrical Communication Laboratory, Nippon Telegraph and Telephone Public Corporation, Tokai-mura, Ibaraki, Japan.

with those for a p^+n Ge APD at both 1.3 and 1.55 μm . In addition, this report presents data from 2 Gbit/s optical transmission experiments with 51.5 km long 1.55 μm dispersion-free fibers, as well as a 1.55 μm optical pulse broadening experiment with 1.3 μm dispersion-free fibers. Future prospects for repeater spacing in PCM-IM single-mode optical fiber transmission systems are also discussed.

II. Ge APD RECEIVER SENSITIVITY

At 1.3 μm , optical receiver sensitivity dependence on the data rate has been studied for PCM-IM optical transmission systems with a Ge APD detector and bipolar transistor and FET front ends [3]. Results show that an optical receiver with a Ge APD and a 50 Ω bipolar transistor front end shows promise for use in long wavelength optical transmission systems having long repeater spacing and a high data rate, at least above 400 Mbit/s. In this section, improved receiver sensitivity at 1.55 μm , achieved by using a reach-through type Ge APD, is described in detail.

High-speed pulse responses of Ge APD's were measured for the purpose of discussing detector performance of a p^+nn^- Ge APD, in comparison with a p^+n Ge APD. A gigabit/s optical transmission system, improved by a GaAs FET laser driver in the transmitter and a tunnel diode comparator in a receiver decision circuit, has previously been reported [3]. A similar optical transmission system configuration was used in this study, except that a 1.55 μm semiconductor laser, 1.55 μm dispersion-free fibers, and a reach-through type Ge APD were employed.

A. High-Speed Pulse Response

Quantum efficiency dependence on wavelength, dark current dependence on avalanche gain, and dark current noise have already been reported in detail, for cases where Ge APD's receive CW optical power [15], [16]. Small signal frequency responses for Ge APD's at 1.55 μm have also been reported [14]. Detector performance, with optical pulse signals, is also important in evaluating the receiver sensitivity of PCM-IM optical receivers. A decrease in pulse response performance degrades the optical receiver sensitivity, mainly at a high data rate.

High-speed pulse response for the photodetector was evaluated in the following way. The optical signal, used in the pulse response measurement, was a return-to-zero (RZ) pulse with a $2^{15}-1$ pseudorandom noise (PN) pulse pattern and 50 percent mark density. The semiconductor laser used as an optical source was modulated under conditions where the modulated optical pulse had a 50 percent duty factor and the optical-signal extinction ratio degradation was negligibly small.

The average APD photocurrent i_{av} generated by the incident light signal with a constant power P_0 is given by

$$i_{av} = \eta \cdot M \cdot P_0 \cdot (e/h\nu). \quad (1)$$

Here η and M are the quantum efficiency and avalanche multiplication factor for the APD as measured with a dc light, and $h\nu/e$ is the photon energy in electron volts. When incident light with average power P_0 is modulated by an RZ pulse

with a 50 percent mark density and 50 percent duty factor, peak photocurrent i_p is given by

$$i_p = \eta \cdot M \cdot R_m \cdot P_0 \cdot (4e/h\nu). \quad (2)$$

Here R_m is a high-speed pulse response factor for the APD and is dependent on pulse modulation rate. The pulse response in the APD's is limited by the transit time for carrier diffusion or drift, as well as by the time needed for carriers to build up the avalanche multiplication. For a nonreach-through type APD, the pulse response mainly depends on the diffusion time for carriers generated in an undepleted region. However, drift time for carriers across the depletion width dominates pulse response in a reach-through type APD. Multiplication buildup time depends on the ionization coefficient ratio of electrons and holes, and also affects the pulse response of an APD.

The generated primary photocurrent is multiplied by M . The multiplied signal photocurrent is led to a preamplifier having input resistor R_L and gain A . The peak voltage for amplified signal v_p is given by

$$v_p = A \cdot R_L \cdot i_p. \quad (3)$$

The product of the quantum efficiency and high-speed pulse response factor is given by

$$\eta \cdot R_m = (1/P_0 \cdot M) \cdot (v_p/4R_L \cdot A) \cdot (h\nu/e). \quad (4)$$

The value $\eta \cdot R_m$ can be calculated by (4) when output peak voltage v_p is observed by the amplifier, and input resistance and amplifier gain are known, and the oscilloscope is calibrated. Output v_p decreases with the pulse response degradation resulting from a tailing, which depends on the incident light wavelength or on the APD bias voltage. The product of quantum efficiency and the pulse response factor $\eta \cdot R_m$ will be used in evaluating the detector responsivity at various data rates.

B. Receiver Sensitivity at 1.3 μm

Optical receiver sensitivities for p^+nn^- and p^+n Ge APD's were measured at 1.3 μm , where Ge APD's showed high detector responsivity. This was done for the purpose of effecting a comparison with sensitivities at 1.55 μm . The optical source was an InGaAsP buried-heterostructure semiconductor laser emitting at 1.303 μm [17]. The laser threshold current I_{th} was 40 mA at 16°C. Fig. 1 shows the Ge APD avalanche multiplication factor dependence on bias at a constant incident light power of -26 dBm. Two Ge APD's have different breakdown voltage values. The reach-through type p^+nn^- Ge APD shows a more gradual increase in avalanche gain when the bias is increased than the p^+n Ge APD. Optical receivers with p^+nn^- Ge APD's are more resistant to temperature and bias voltage fluctuations than optical receivers with p^+n Ge APD's.

Pulse response in two types of Ge APD's was measured at 1.3 μm . The dependence of the product $\eta \cdot R_m$ on the avalanche multiplication factor at 1 and 2 Gbit/s data rates is shown in Fig. 2. Quantum efficiencies η for p^+nn^- and p^+n Ge APD's are 80 percent and 60 percent, respectively. At 1 Gbit/s,

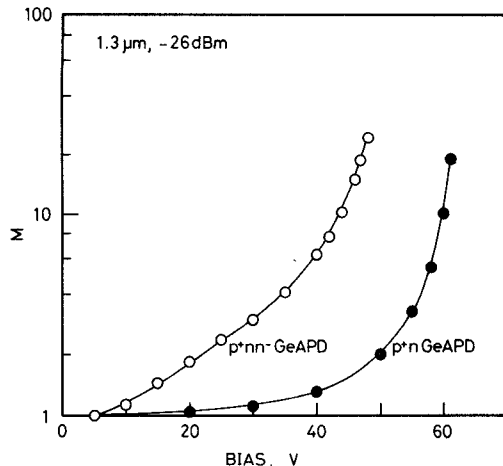


Fig. 1. Ge APD avalanche multiplication factor M dependence on bias at $1.3 \mu\text{m}$. Incident light power is -26 dBm .

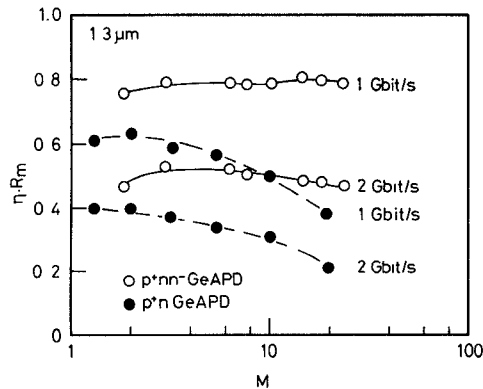


Fig. 2. Dependence of product of quantum efficiency and high-speed pulse response factor $\eta \cdot R_m$ on avalanche multiplication factor at $1.3 \mu\text{m}$.

$\eta \cdot R_m$ for each Ge APD with a low avalanche gain is almost equal to η . The p^+nn^- Ge APD has a pulse response independent of the avalanche multiplication factor M beyond the reach-through voltage of about 20 V. On the other hand, the R_m for the p^+n Ge APD becomes lower at a high M value. Pulse response degradation at a high M seems to be caused mainly by the buildup time for avalanche multiplication. This is because the ionization coefficient ratio value for the p^+n Ge APD is almost unity, as presumed by its avalanche excess noise factor. When a 2 Gbit/s optical signal is used, the product $\eta \cdot R_m$ at a low M is 2 dB worse than the η , for both types of Ge APD's. Taking account of the difference in $\eta \cdot R_m$ values for two Ge APD's, it is expected that at $1.3 \mu\text{m}$ an optical receiver with a p^+nn^- Ge APD will have 2 dB more sensitivity than one with a p^+n Ge APD.

Fig. 3 shows the dependence of $1.3 \mu\text{m}$ optical receiver sensitivity on data rates ranging from 400 Mbit/s to 2 Gbit/s. Solid lines are theoretical values calculated from Personick's theory [18]. The laser modulation current was optimized at each data rate by minimizing the error rate under conditions of constant optical power reception. The required optical power level for a 10^{-9} error rate is -33.4 dBm at 2 Gbit/s for the p^+nn^- Ge APD. This level is 1.5 dB lower than for a p^+n Ge APD. Experimental results show that the high-speed

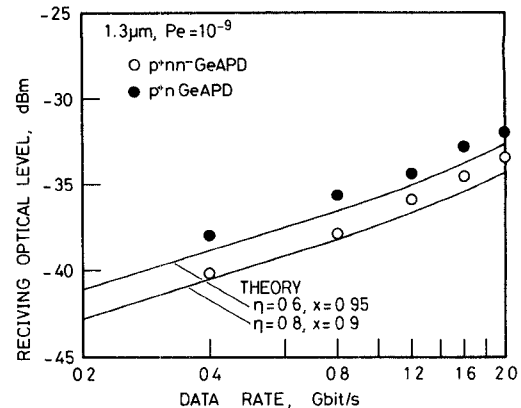


Fig. 3. $1.3 \mu\text{m}$ optical receiver sensitivity dependence on data rate.

pulse response in the photodetector is an effective indicator of the optical receiver sensitivity.

C. Receiver Sensitivity at $1.55 \mu\text{m}$

High-speed pulse response for the p^+nn^- and p^+n Ge APD's at 0.4, 1, and 2 Gbit/s was measured at $1.55 \mu\text{m}$, where silica optical fibers have minimum loss. The optical source was an InGaAsP buried-heterostructure semiconductor laser emitting at $1.550 \mu\text{m}$ [19]. The threshold current was 73 mA at 19.5°C . The avalanche multiplication factor M for Ge APD's is plotted against the detector bias voltage at a constant incident optical power of -26 dBm in Fig. 4. Multiplication characteristics for Ge APD's at $1.55 \mu\text{m}$ are similar to those for $1.3 \mu\text{m}$ that were shown in Fig. 1. The avalanche gain factor at $1.55 \mu\text{m}$, however, was slightly larger than that at $1.3 \mu\text{m}$. Characteristics for the Ge APD's used in this study are summarized in Table I. Both types of Ge APD's have lower quantum efficiency, but also a lower avalanche excess noise factor x at $1.55 \mu\text{m}$ than they have at $1.3 \mu\text{m}$. The p^+nn^- Ge APD is superior to the p^+n Ge APD at each wavelength.

Fig. 5 shows eye patterns for the receiver at 0.4, 1, and 2 Gbit/s. The upper and lower traces represent photocurrent signals for the p^+nn^- and p^+n Ge APD's, respectively. At 400 Mbit/s, the semiconductor laser was modulated by the pulse signal current I_p of 60 mA_{0-p} which was superimposed on a bias current I_{dc} of 57 mA. An I_{dc} of 66 mA and I_p of 56 mA_{0-p} were chosen at 1 and 2 Gbit/s to give the optimum error rate performance. Multiplication factors for the p^+nn^- and p^+n Ge APD's at $1.55 \mu\text{m}$ were 15 and 10, respectively. Fig. 5(a) shows that relaxation oscillation, which exists in the p^+nn^- Ge APD response, was not observed in the eye pattern received by the p^+n Ge APD. Jitter in the pulse leading edge is worse for the p^+n Ge APD than for the p^+nn^- Ge APD at 1 Gbit/s. The 2 Gbit/s eye pattern waveform for the p^+n Ge APD has a longer pulse tailing edge than that for the p^+nn^- Ge APD. These experimental results show that the reach-through p^+nn^- Ge APD is a great improvement with respect to the high-speed optical pulse response.

Fig. 6 shows the dependence of $\eta \cdot R_m$ product on M , as measured for the p^+nn^- and p^+n Ge APD's at 0.4, 1, and 2 Gbit/s. Quantum efficiencies η at $1.55 \mu\text{m}$ are 60 percent for the p^+nn^- type, and 40 percent for the p^+n type. The experimental $\eta \cdot R_m$ value for each Ge APD is degraded in

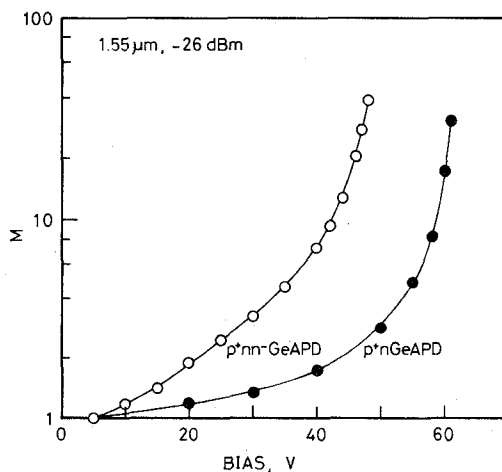


Fig. 4. Dependence of Ge APD avalanche multiplication factor M on bias at $1.55 \mu\text{m}$. Incident light power is -26 dBm .

TABLE I
Ge APD CHARACTERISTICS

Type	$p^{+}nn^{-}$	$p^{+}n$	
Wavelength (μm)	1.3	1.55	1.3
Quantum efficiency, η	0.8	0.6	0.6
Excess noise factor, x	0.9	0.83	0.95
Sensitive area diameter (μm)	80		100
Capacitance (pF)	0.6		1.5
Breakdown voltage (V)	49		62

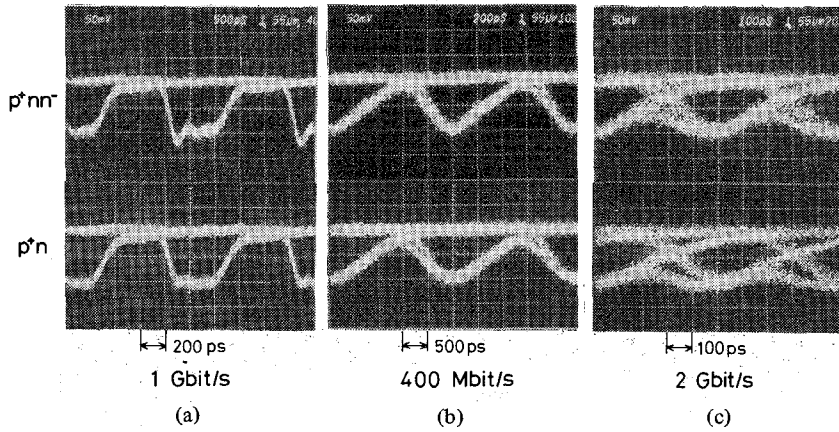


Fig. 5. Received eye patterns with RZ waveform. Upper and lower traces respectively represent signals for a $p^{+}nn^{-}$ and $p^{+}n$ Ge APD's. Data rates are (a) 400 Mbit/s, (b) 1 Gbit/s, and (c) 2 Gbit/s.

comparison with η , even at 400 Mbit/s, even though at 1 Gbit/s, the $1.3 \mu\text{m} \eta \cdot R_m$ is close to η . The $1.55 \mu\text{m}$ optical receiver with a $p^{+}nn^{-}$ Ge APD was expected to have a receiver sensitivity improvement of 1.3 dB over that with a $p^{+}n$ Ge APD at 400 Mbit/s. At 2 Gbit/s, however, the $p^{+}nn^{-}$ Ge APD provides an optical receiver sensitivity 3 dB better than for the $p^{+}n$ Ge APD, when the eye pattern degradation at the

sampling point for decision, shown in Fig. 5(c), is evaluated. Since the undesirable carriers injection into the avalanche region at $1.55 \mu\text{m}$ is reduced, the pulse response degradation due to the multiplication process time is improved. Experimental results for the pulse response measurement of Ge APD's at 1.55 and $1.3 \mu\text{m}$ are summarized in Table II.

Experimental results showing $1.55 \mu\text{m}$ optical receiver

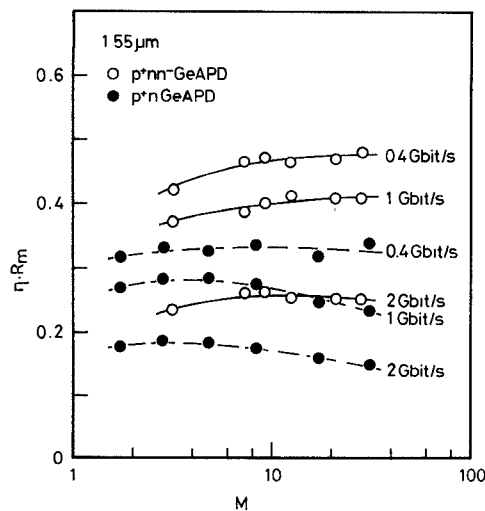


Fig. 6. Dependence of product of quantum efficiency and high-speed pulse response factor $\eta \cdot R_m$ on avalanche multiplication factor at $1.55 \mu\text{m}$.

TABLE II
EXPERIMENTAL PULSE RESPONSE RESULTS FOR Ge APD's

Type	$p^{+}nn^{-}$	$p^{+}n$		
Wavelength (μm)	1.3	1.55	1.3	1.55
η	0.8	0.6	0.6	0.4
$\eta \cdot R_m^*$ at 400 Mbit/s	—	0.46	—	0.34
at 1 Gbit/s	0.80	0.40	0.39	0.27
at 2 Gbit/s	0.49	0.26	0.21	0.17

* $M = 20$

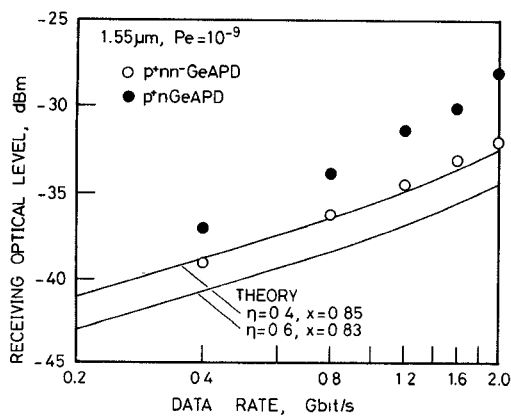


Fig. 7. Dependence of $1.55 \mu\text{m}$ optical receiver sensitivity on data rate.

sensitivity at various data rates are shown in Fig. 7. Solid lines are theoretical values. 2 Gbit/s optical receiving levels at a 10^{-9} error rate are -32.0 dBm for the $p^{+}nn^{-}$ Ge APD, and -28.0 dBm for the $p^{+}n$ Ge APD, respectively. Detector sensitivity for the $p^{+}nn^{-}$ Ge APD is 4 dB superior to that for the $p^{+}n$ Ge APD, as is expected from the results coming from high-speed pulse response measurement. The difference between experimental and theoretical receiver sensitivity at

$1.55 \mu\text{m}$ is greater than that at $1.3 \mu\text{m}$. The large degradation from the theoretical values at $1.55 \mu\text{m}$ is caused by the degraded pulse response shown in Fig. 6. The sensitivity for the $p^{+}nn^{-}$ Ge APD is in good agreement with the theoretical values when $\eta = 0.4$. The experimental results at $1.55 \mu\text{m}$ also show that high-speed pulse response factor R_m is effective for looking at high data rate detector responsivity in optical receiver system design.

Optical receiving levels at a 10^{-9} error rate for the $p^{+}nn^{-}$ and $p^{+}n$ Ge APD's are summarized in Table III. Optical sensitivity for the improved Ge APD at $1.55 \mu\text{m}$ is 1.5 dB worse than that at $1.3 \mu\text{m}$. Development of a highly responsive APD with a $\eta \cdot R_m$ product of 60 percent at $1.55 \mu\text{m}$ will remove the receiver sensitivity difference between 1.3 and $1.55 \mu\text{m}$.

III. SINGLE-MODE FIBER TRANSMISSION AT $1.55 \mu\text{m}$

In order to characterize long-span single-mode fiber transmission, $1.55 \mu\text{m}$ optical pulse transmission experiments were carried out using 1.55 and $1.3 \mu\text{m}$ dispersion-free fibers. Optical pulse broadening and 2 Gbit/s transmission characteristics will be discussed in this section in some detail.

A. $1.3 \mu\text{m}$ Dispersion-Free Fiber

$1.3 \mu\text{m}$ dispersion-free fibers used in the experiment were fabricated by the MCVD method [20]. The fibers, with a SiO_2 - GeO_2 core and pure SiO_2 cladding, typically were about 5 km unit length. Fibers with silicone buffer coating were loosely wound on drums. Eight fiber strands were spliced by the fusion splice method [21]. Core diameter and relative index difference were $11 \mu\text{m}$ and 0.2 percent on the average, respectively [3]. Total fiber length was 44.3 km. Overall loss for the fiber, including splice loss, was 17.7 dB at $1.55 \mu\text{m}$.

To test pulse broadening in the fiber, the $1.55 \mu\text{m}$ semiconductor laser was modulated by an isolated pulse with 1/24 mark density at 2 Gbit/s. The modulating currents I_p and I_{dc} were 56 mA_{0-p} and 66 mA , respectively. The laser output spectrum is shown in Fig. 8. The laser emitted in multi-longitudinal modes, since I_{dc} was selected to be below the threshold value of 73 mA. Full width at half maximum of the laser output spectrum was about 7 nm. Longitudinal mode spacing was 1.6 nm.

Fig. 9 shows optical pulse broadening for 1 m, 5.2, 11.7, 23.9, 33.7, and 43.3 km long fibers. These photographs show behavior for optical pulse transmission through a dispersive line. Fiber dispersion causes different group delay values for each longitudinal mode. Multiple pulses, corresponding to longitudinal modes with a broadened envelope, were observed when the fibers were longer than about 20 km. Fiber dispersion at $1.55 \mu\text{m}$ was derived to be $18 \text{ ps}/(\text{km} \cdot \text{nm})$, from the separated pulse interval, longitudinal mode spacing, and fiber length [9]. The asymmetrical envelope for the pulse waveform, shown in Fig. 9(c) and (d), is due to the laser output spectral shape. This optical pulse broadening result shows that $1.3 \mu\text{m}$ dispersion-free fibers can afford only a repeater spacing of only a few km at $1.55 \mu\text{m}$ with transmission of 2 Gbit/s information.

TABLE III
OPTICAL RECEIVING LEVEL AT 10^{-9} ERROR RATE

Type	$p^+ nn^-$	$p^+ n$	
Wavelength (μm)	1.3	1.55	1.3
Optical level (dBm)			1.55
at 400 Mbit/s	-40.2	-39.0	-38.0
at 800 Mbit/s	-37.9	-36.2	-35.6
at 1.2 Gbit/s	-35.9	-34.4	-33.4
at 1.6 Gbit/s	-34.5	-33.0	-32.8
at 2 Gbit/s	-33.4	-32.0	-31.9

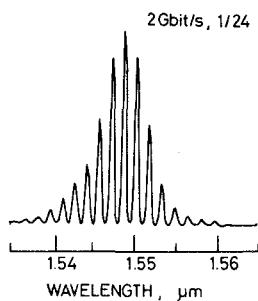


Fig. 8. Output spectrum for $1.55 \mu\text{m}$ semiconductor laser modulated by isolated pulse with $1/24$ mark density at 2 Gbit/s . $I_{dc} = 66 \text{ mA}$, $I_p = 56 \text{ mA}_0 - p$, and $I_{th} = 73 \text{ mA}$.

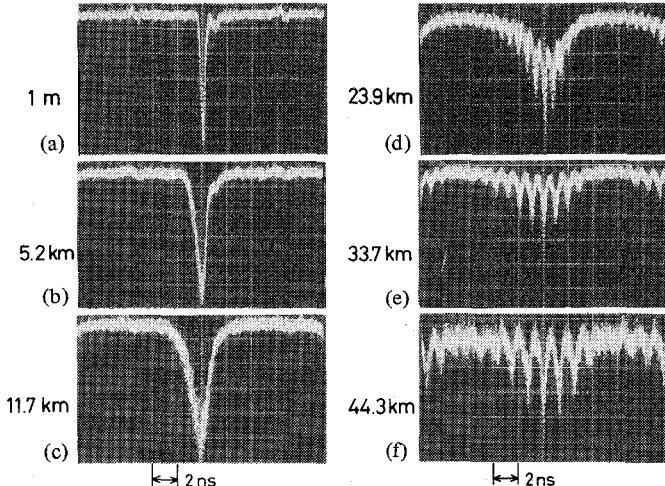


Fig. 9. Dependence of $1.55 \mu\text{m}$ optical pulse broadening on $1.3 \mu\text{m}$ dispersion-free fiber length. Fiber lengths are (a) 1 m, (b) 5.2 km, (c) 11.7 km, (d) 23.9 km, (e) 33.7 km, and (f) 44.3 km.

Fig. 10 shows optical pulse waveforms corresponding to one longitudinal mode separated from the other by the fiber dispersion. After pulses are sufficiently separated in time, each optical pulse included only one longitudinal mode power. The width of the optical pulse, corresponding to a certain longitudinal mode, remains almost the same as that for a 1 m transmission, as can be seen in Fig. 10(d)-(f), after transmission over 23.9 km or more. This result confirms that a single frequency optical source is necessary for transmitting high-

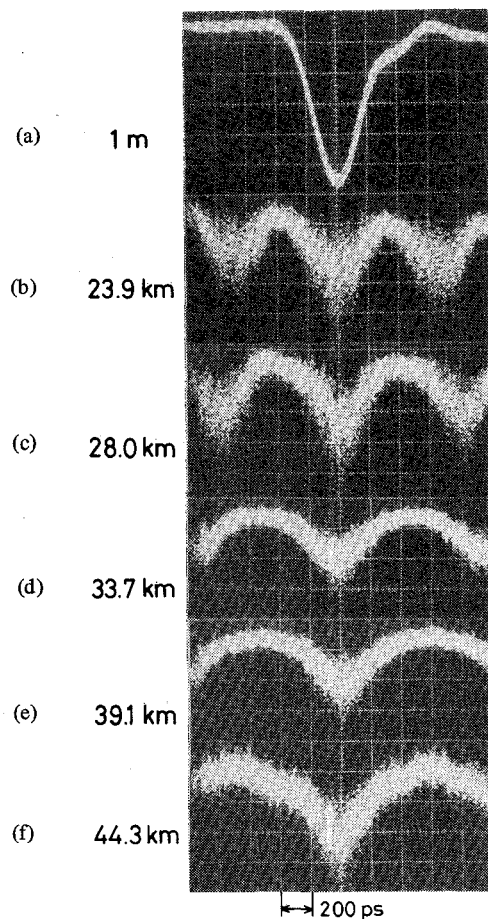


Fig. 10. $1.55 \mu\text{m}$ optical pulse waveforms separated by fiber dispersion in $1.3 \mu\text{m}$ dispersion-free fibers. Fiber lengths are (a) 1 m, (b) 23.9 km, (c) 28.0 km, (d) 33.7 km, (e) 39.1 km, and (f) 44.3 km.

speed optical pulse signals at $1.55 \mu\text{m}$ through the $1.3 \mu\text{m}$ dispersion-free fibers.

B. $1.55 \mu\text{m}$ Dispersion-Free Fiber

By using dispersion-free fibers at $1.5 \mu\text{m}$, an optical transmission experiment was previously carried out successfully at 800 Mbit/s with 20 km repeater spacing [22]. The fibers, fabricated by the MCVD method, had a relative index difference of 0.55 percent, and a core diameter of $4.4 \mu\text{m}$. The overall zero-dispersion wavelength for a spliced 20 km fiber span was $1.48 \mu\text{m}$. Average fiber loss, including splice loss, was 1.2 dB/km at $1.5 \mu\text{m}$.

In the present study, $1.55 \mu\text{m}$ dispersion-free fibers were prepared by the VAD method. Three fiber strands, of 28.5, 20.0, and 3.0 km in length, were fusion-spliced. The relative index difference was about 0.7 percent, and the core diameter was about $4.5 \mu\text{m}$. The fibers, with a SiO_2 - GeO_2 core and pure SiO_2 cladding, were loosely wound on drums after a silicone coating. The total length and overall average fiber loss, including splice loss, were 51.5 km and 0.54 dB/km at $1.55 \mu\text{m}$. The best fiber used in this study had 0.4 dB/km loss and 20.0 km length. The fibers showed improvement in the form of reduced fiber loss and ease in accurately establishing the zero-dispersion wavelength.

Laser output power was coupled into the $1.55 \mu\text{m}$ dispersion-

free fibers by a hemispherical microlens tipped on the single-mode fiber end [23]. Optical coupling loss of 4.5 dB was achieved by a microlens having a 7 μm radius and that was optimumly separated 6 μm from the laser. Coupling loss included splice loss between a single-mode fiber with the microlens and the 1.55 μm dispersion-free fibers. A 5 dB improvement over the butt joint method was achieved.

Fig. 11 shows received optical pulses transmitted through 1 m, 28.5 km, and 51.5 km fibers in the pulse broadening experiment with the 1.55 μm dispersion-free fibers. The optical detector used was the reach-through type p^+nn^- Ge APD. The 1.55 μm laser output spectrum had the same shape as was shown in Fig. 8, and had a 7 nm width. Low optical output power after 51.5 km transmission caused a decrease in signal-to-noise ratio, as shown in Fig. 11(c). Although the semiconductor laser oscillated in multilongitudinal modes with full spectral width at a half maximum of about 7 nm, no degradation occurred in the received optical pulse waveform even after 51.5 km fiber transmission. If a measurement error of 10 ps is assumed, fiber dispersion is at most 0.2 ps/(km \cdot nm) at 1.55 μm . The low dispersion degradation indicates that the overall zero-dispersion wavelength for the fibers is in good agreement with the 1.55 μm laser output wavelength.

C. 2 Gbit/s Transmission Experiment

Fig. 12 shows 2 Gbit/s error rate characteristics at 1.55 μm . This figure also shows experimental results obtained with a receiver employing a p^+n Ge APD and 1-m-long single-mode fiber. This is in order to show the receiver sensitivity improvement. The solid line is the theoretical curve. The optical receiving level at a 10^{-9} error rate was -31.4 dBm after 51.5 km transmission for the p^+nn^- Ge APD receiver. Only 0.6 dB impairment occurred, which could be seen to be caused by the long-span fiber transmission, when compared with the receiving level after 1 m transmission for the same receiver.

The 1.55 μm laser was directly modulated by a pulse current where $I_p = 56 \text{ mA}_0 - p$ at 2 Gbit/s was superimposed on a bias of $I_{dc} = 66 \text{ mA}$ (which was below the threshold $I_{th} = 73 \text{ mA}$). The semiconductor laser, directly modulated by a pseudorandom noise pulse pattern, had an output spectrum with multilongitudinal modes, as is shown in Fig. 13. Fig. 14 shows 2 Gbit/s eye pattern waveforms received after 1 m and 51.5 km transmission. Although there is no pulse broadening caused by fiber dispersion, in spite of multilongitudinal mode laser emission, the eye pattern waveform received after 51.5 km transmission had more jitter than that after 1 m transmission. Jitter increase caused an 0.6 dB optical power penalty in the error rate characteristics, since the decision circuit in the optical receiver had a narrow timing margin at the 2 Gbit/s pulse rate.

Fig. 15 shows an optical power level diagram for the 2 Gbit/s transmission system with 1.55 μm dispersion-free fibers. Output for the 1.55 μm laser was $+2.3$ dBm on the average, under optimized laser modulation conditions. The level of the optical signal launched into the fiber was -2.2 dBm. A repeater gain of 29.2 dB was achieved in the 2 Gbit/s optical transmission system at 1.55 μm , taking into account the receiving optical level of -31.4 dBm required for a 10^{-9} error

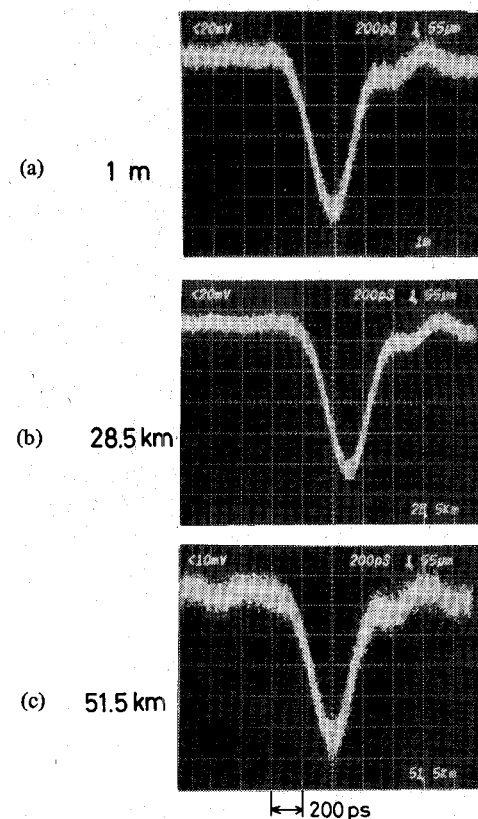


Fig. 11. 1.55 μm optical pulse signals received after 1.55 μm dispersion-free fiber transmissions. Fiber lengths are (a) 1 m, (b) 28.5 km, and (c) 51.5 km.

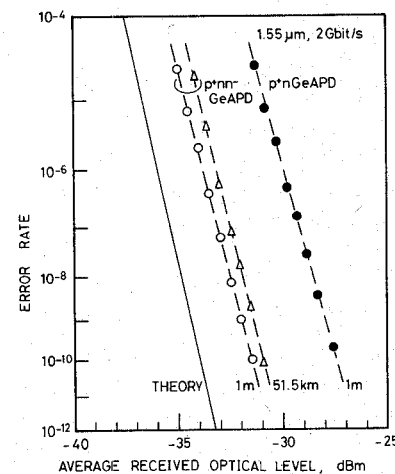


Fig. 12. 2 Gbit/s error rate characteristics at 1.55 μm . Solid line is theoretical value.

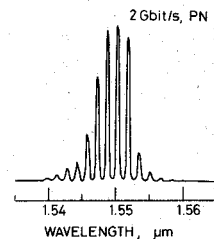


Fig. 13. Output spectrum for 1.55 μm semiconductor laser modulated by PN pulse pattern at 2 Gbit/s. $I_{dc} = 66 \text{ mA}$, $I_p = 56 \text{ mA}_0 - p$, and $I_{th} = 73 \text{ mA}$.

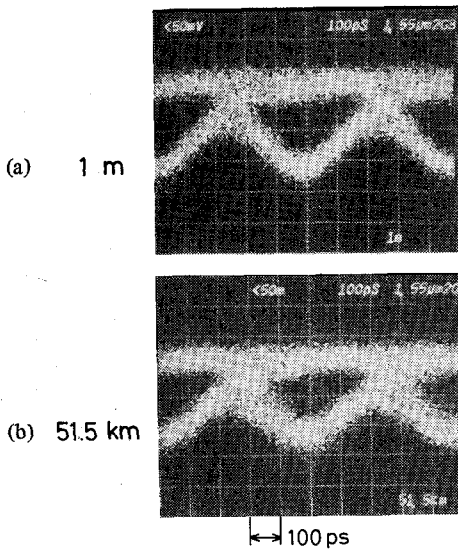


Fig. 14. Received eye pattern waveforms at 2 Gbit/s. Fiber transmission lengths are (a) 1 m and (b) 51.5 km.

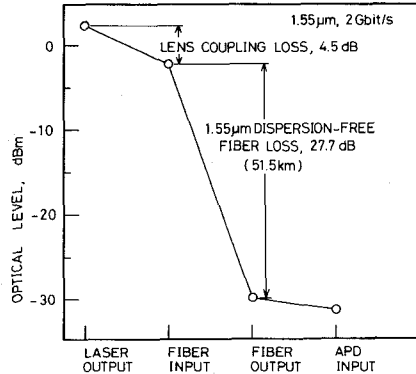


Fig. 15. Optical power level diagram for 2 Gbit/s transmission system with 1.55 μm dispersion-free fibers.

rate. This system has a data rate repeater-spacing product of $103 (\text{Gbit/s}) \cdot \text{km}$.

IV. DISCUSSION AND FUTURE PROSPECTS

The wavelength dependence for dispersion in the 1.55 and 1.3 μm dispersion-free fibers used in this study is shown in Fig. 16. Solid lines are theoretical values calculated by taking into account each fiber parameter [24]. Experimental results were derived from the frequency spectrum [25], pulse broadening [10], and pulse separation [9] for the optical signals received after long-span fiber transmission. The pulse broadening method was based on the difference between pulse widths before and after fiber transmission. The method utilizing pulse separation caused by the fiber dispersion was mentioned in Section III-A. The frequency spectrum shape for the optical signals received after long transmission is also effective for measuring fiber dispersion. Since the experimental values are in good agreement with the theoretical curve, it is confirmed that baseband characteristics in single-mode fibers can be precisely calculated from Gloge's theory.

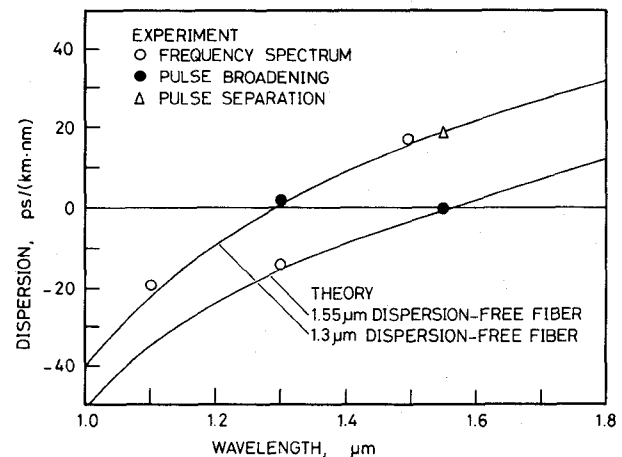


Fig. 16. Fiber dispersion dependence on wavelength for 1.55 and 1.3 μm dispersion-free fibers.

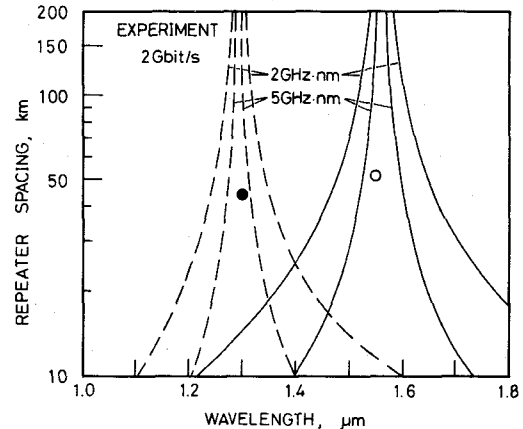


Fig. 17. Dependence of dispersion limited repeater spacing on wavelength. Solid and broken lines respectively represent theoretical results for 1.55 and 1.3 μm dispersion-free fibers.

Fig. 17 shows repeater spacing as determined by the dispersion in two types of single-mode optical fibers. The repeater spacing is assumed to be limited only by the transmission bandwidth caused by fiber dispersion. Fiber parameters for 1.55 and 1.3 μm dispersion-free fibers reported in the previous sections were used in calculating theoretical fiber dispersion. Fiber bandwidth is decided by the product of laser spectral width and fiber dispersion [10]. Solid and broken lines respectively represent theoretical repeater spacing for 1.55 and 1.3 μm dispersion-free fibers. The parameter used in Fig. 17 is the product of a 3 dB bandwidth (as required by the transmission systems) and the full width at half maximum for the laser output spectrum. Each single-mode fiber has an extremely wide bandwidth near its zero dispersion wavelength. When the laser output wavelength is matched with the zero-dispersion wavelength for a single-mode fiber, repeater spacing in the optical transmission system is limited by the fiber loss. Repeater spacing limits due to fiber loss are not shown in Fig. 17, but will be discussed later. Two plotted data results represent 2 Gbit/s optical transmission experiment at 1.55 and 1.3 μm [3]. The repeater spacing in these experiments was

not limited by fiber dispersion, but by fiber loss. This figure presents permissible wavelength deviation for the laser transmitter, as limited by repeater spacing and data rate in the transmission system. 1.55 μm dispersion-free fibers have a wider permissible wavelength region than 1.3 μm dispersion-free fibers, under the same repeater spacing and data rate conditions.

Subsequent to matching between the laser and zero-dispersion wavelengths, repeater spacing is limited by only fiber loss. Fig. 18 shows the dependence of theoretical repeater spacing on data rate for PCM-IM single-mode optical fiber transmission systems. In calculating repeater spacing, it is assumed that the optical power input into the single-mode fiber is 0 dBm, that the quantum efficiency and excess noise factor for the APD are 80 percent and 0.8 at 1.55 μm , and that the system margin is 3 dB. Solid and broken lines indicate the repeater spacing limited by fiber loss and dispersion, respectively. The product of fiber dispersion and laser output spectral width is used as a parameter, and represents the bandwidth determined by the fiber dispersion. Repeater spacings for 2 Gbit/s transmission experiments at 1.55 and 1.3 μm are below the theoretical loss limit value, with the larger fiber loss, and repeater gain smaller by 6 dB in the experimental systems than in the values used in the theoretical study, taken into account.

1.3 μm dispersion-free fiber, with losses of 0.35 dB/km at 1.3 μm and 0.2 dB/km at 1.55 μm , has been reported [26]. The present 2 Gbit/s transmission system has a 31 dB repeater gain at 1.3 μm . It is expected that 2 Gbit/s transmission system with 1.3 μm dispersion-free fibers has about 60 km repeater spacing assuming a 3 dB system margin and an excess fiber loss of 0.1 dB/km.

The lowest loss value for 1.55 μm dispersion-free fibers is 0.35 dB/km at 1.55 μm . However, the 1.55 μm dispersion-free fiber loss can be reduced to 0.25 dB/km by a design with lower relative index difference [11]. In the present transmission system, optical receiver sensitivity at 1.55 μm is 1.5 dB worse than at 1.3 μm . The transmission system presented in this study has 29 dB repeater gain at 1.55 μm . Development of 1.55 μm dispersion-free fiber with a 0.25 dB/km fiber loss and 0.1 dB/km excess loss will bring about 2 Gbit/s optical transmission systems having 12 km longer repeater spacing or a 4 dB larger system margin than with 1.3 μm dispersion-free fibers. In the present system with an InGaAsP semiconductor laser and p^+nn^- Ge APD, fiber input level and optical receiver sensitivity at 1.55 μm are slightly inferior to those at 1.3 μm . Transmitting and receiving performance of 1.55 μm optical devices will be improved in the near future, as realized at 1.3 μm . The system performance improvement will further expand the advantage of operating at 1.55 μm .

Furthermore, realization of a single frequency optical source, that operates stably and has its undesirable modes extremely reduced under direct modulation, will enable transmission of a 1.55 μm high-speed optical signal through long-span 1.3 μm dispersion-free fibers [10]. Repeater spacing for the 2 Gbit/s transmission system can then be extended to more than 100

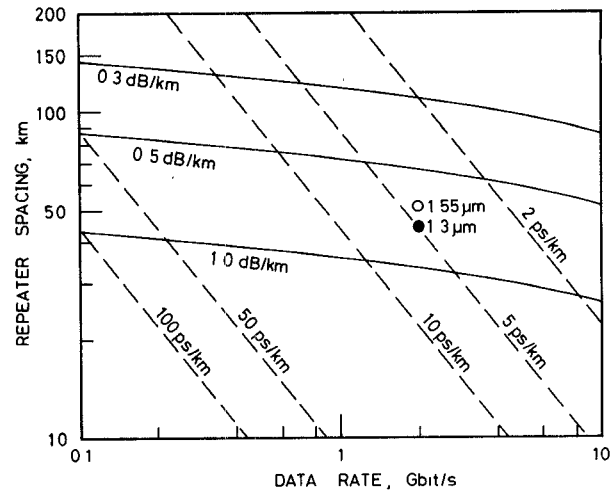


Fig. 18. Dependence of theoretical repeater spacing on data rate for PCM-IM optical fiber transmission systems. Solid and broken lines are theoretical results limited by fiber loss and fiber dispersion, respectively.

km, assuming even an excess fiber loss of 0.1 dB/km. Realization of an optical digital transmission system, with a data rate repeater-spacing product of 200 (Gbit/s) · km, seems to depend on whether a single frequency optical source at 1.55 μm and a high-speed, high-efficiency, and low-noise APD can be fabricated.

V. CONCLUSION

Receiver sensitivity characteristics for optical receivers having a Ge APD and 50 Ω Si bipolar transistor front end, as well as long-span single-mode fiber transmission characteristics were studied at 1.55 μm , where silica fibers have minimum loss. High-speed pulse response and optical receiver sensitivity in an optical receiver with a new reach-through type p^+nn^- Ge APD at 1.55 and 1.3 μm were measured at data rates ranging from 400 Mbit/s to 2 Gbit/s. These results were compared with those for a conventional p^+n Ge APD. The product of quantum efficiency and high-speed pulse response factor, $\eta \cdot R_m$, for the p^+nn^- Ge APD at 1.55 μm was 46 percent at 400 Mbit/s, 40 percent at 1 Gbit/s, and 26 percent at 2 Gbit/s, in spite of the quantum efficiency η of 60 percent. The p^+nn^- Ge APD had higher detector responsivity than the p^+n Ge APD. The 2 Gbit/s optical power level at a 10^{-9} error rate for the p^+nn^- Ge APD was -32.0 dBm at 1.55 μm . This was a 4 dB improvement over the p^+n Ge APD receiver, as was expected from the experimental results involving pulse response measurement. Since the high-speed pulse response factor R_m reveals that detector responsivity depends on pulse rate, this R_m is effective in discussing detector performance in PCM-IM optical transmission systems. For the experimental system used, optical sensitivity at 1.55 μm was only 1.5 dB worse than at 1.3 μm .

A 2 Gbit/s optical transmission experiment at 1.55 μm was effected by using 1.55 μm dispersion-free fibers 51.5 km long having a 0.54 dB/km average loss. The required optical power level for a 10^{-9} error rate was -31.4 dBm for 51.5 km transmission. There was only 0.6 dB impairment caused by

jitter increase in the received signals. A 29.2 dB repeater gain, and low-loss dispersion-free fibers in the system, were used in an optical fiber transmission experiment that achieved a data rate repeater-spacing product of 103 (Gbits/s) · km. Results in the 1.55 μm pulse broadening experiment showed that a single frequency optical source is necessary for transmitting high-speed optical signals at 1.55 μm through 1.3 μm dispersion-free fiber.

Future prospects for repeater spacing with PCM-IM single-mode fiber transmission systems were discussed, taking into account the results from the 2 Gbit/s transmission experiment and fiber dispersion measurements. The present transmission system with 1.55 μm dispersion-free fibers offers slight performance improvement over the system with 1.3 μm dispersion-free fibers, although, at 1.55 μm , a single-mode fiber loss is 0.54 dB/km and repeater gain is 2 dB smaller than that at 1.3 μm . Low-loss 1.55 μm dispersion-free fibers with 0.25 dB/km loss can bring about 12 km longer repeater spacing or a 4 dB larger system margin, and a wider permissible laser wavelength region than 1.3 μm dispersion-free fibers. Further, development of a stably operating single-frequency optical source at 1.55 μm , and a high-speed, highly efficient and low-noise APD will bring about 2 Gbit/s optical fiber transmission systems with repeater spacings of more than 100 km.

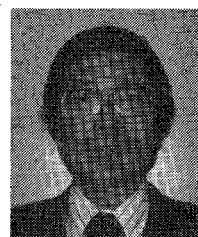
ACKNOWLEDGEMENT

The authors would like to thank H. Kanbe, S. Machida, and N. Imoto for fruitful discussions, and N. Inagaki, M. Nakahara, and T. Ikegami for encouragement.

REFERENCES

- [1] T. Kimura and K. Diakoku, "A proposal on optical fiber transmission systems in a low-loss 1-1.4 μm wavelength region," *Opt. Quantum Electron.*, vol. 9, pp. 33-42, Jan. 1977.
- [2] D. E. Payne and W. A. Gambling, "Zero material dispersion in optical fiber," *Electron. Lett.*, vol. 11, pp. 176-178, Apr. 1975.
- [3] J. Yamada and T. Kimura, "Characteristics of Gbit/s optical receiver sensitivity and long-span single-mode fiber transmission at 1.3 μm ," *IEEE J. Quantum Electron.*, vol. QE-18, pp. 718-727, Apr. 1982.
- [4] T. Miya, T. Terunuma, T. Hosaka, and T. Miyashita, "An ultimate low-loss single-mode fiber at 1.55 μm ," *Electron. Lett.*, vol. 15, pp. 106-108, Feb. 1979.
- [5] N. Imoto, A. Kawana, S. Machida, and H. Tsuchiya, "Characteristics of dispersion free single-mode fiber in the 1.5 μm wavelength region," *IEEE J. Quantum Electron.*, vol. QE-16, pp. 1052-1058, Oct. 1980.
- [6] O. Mikami, "1.55 μm GaInAsP distributed feedback lasers," *Japan. J. Appl. Phys.*, vol. 20, pp. L488-L490, July 1981.
- [7] T. Matsuoka, H. Nagai, Y. Itaya, Y. Noguchi, Y. Suzuki, and T. Ikegami, "CW operation of DFB-BH GaInAsP/InP lasers in 1.5 μm wavelength region," *Electron. Lett.*, vol. 18, pp. 27-28, Jan. 1982.
- [8] K. Utaka, K. Kobayashi, F. Koyama, Y. Abe, and Y. Suematsu, "Single-wavelength operation of 1.53 μm GaInAsP/InP buried-heterostructure integrated twin-guide laser with distributed Bragg reflector under direct modulation up to 1 GHz," *Electron. Lett.*, vol. 17, pp. 368-369, May 1981.
- [9] J. Yamada, S. Kobayashi, H. Nagai, and T. Kimura, "Modulated single-longitudinal mode semiconductor laser and fiber transmission characteristics at 1.55 μm ," *IEEE J. Quantum Electron.*, vol. QE-17, pp. 1006-1009, June 1981.
- [10] J. Yamada, S. Machida, T. Mukai, H. Tsuchiya, and T. Kimura, "Long-span single-mode fiber transmission characteristics in long wavelength region," *IEEE J. Quantum Electron.*, vol. QE-16, pp. 874-884, Aug. 1980.
- [11] S. Tomaru, M. Kawachi, M. Yasu, T. Miya, and T. Edahiro, "VAD single-mode fiber with high Δn values," *Electron. Lett.*, vol. 17, pp. 731-732, Oct. 1981.
- [12] T. Izawa, S. Sudo, and F. Hanawa, "Continuous fabrication process for high-silica fiber preforms," *Trans. IECE Japan*, vol. E62, pp. 779-785, Nov. 1979.
- [13] T. Kaneda, H. Fukada, T. Mikawa, Y. Banba, Y. Toyama, and H. Ando, "Shallow-junction p⁺-n germanium avalanche photodiodes (APD's)," *Appl. Phys. Lett.*, vol. 34, pp. 866-868, June 1979.
- [14] T. Mikawa, S. Kagawa, T. Kaneda, and T. Sakurai, "A reach-through germanium APD for 1.55 μm optical communication systems," *Tech. Rep. IECE Japan*, OQE 81-87, 1981 (in Japanese).
- [15] H. Ando, H. Kanbe, T. Kimura, T. Yamaoka, and T. Kaneda, "Characteristics of germanium avalanche photodiodes in wavelength region of 1-1.6 μm ," *IEEE J. Quantum Electron.*, vol. QE-14, pp. 804-810, Nov. 1978.
- [16] H. Kanbe, G. Grosskopf, O. Mikami, and S. Machida, "Dark current noise characteristics and their temperature dependence in germanium avalanche photodiode," *IEEE J. Quantum Electron.*, vol. QE-17, pp. 1534-1539, Aug. 1981.
- [17] M. Hirao, A. Doi, S. Tsuji, M. Nakamura, and K. Aiki, "Fabrication and characterization of narrow stripe InGaAsP/InP buried heterostructure lasers," *J. Appl. Phys.*, vol. 51, pp. 4539-4540, Aug. 1980.
- [18] S. D. Personick, "Receiver design for digital fiber optic communication system, I and II," *Bell Syst. Tech. J.*, vol. 52, pp. 843-886, July-Aug. 1973.
- [19] H. Nagai, Y. Noguchi, K. Takahei, Y. Toyoshima, and G. Iwane, "InP/GaInAsP buried heterostructure lasers of 1.5 μm region," *Japan. J. Appl. Phys.*, vol. 19, pp. L218-L220, Apr. 1980.
- [20] M. Kawachi, A. Kawana, and T. Miyashita, "Low-loss single-mode fiber at the material-dispersion-free wavelength of 1.27 μm ," *Electron. Lett.*, vol. 13, pp. 442-443, July 1977.
- [21] I. Hatakeyama and H. Tsuchiya, "Fusion splices for single-mode optical fibers," *IEEE J. Quantum Electron.*, vol. QE-14, pp. 614-619, Aug. 1978.
- [22] J. Yamada, S. Machida, T. Mukai, and T. Kimura, "800 Mbit/s optical transmission experiments with dispersion-free fibers at 1.5 μm ," *Electron. Lett.*, vol. 16, pp. 115-117, Feb. 1980.
- [23] J. Yamada, Y. Murakami, J. Sakai, and T. Kimura, "Characteristics of a hemispherical microlens for coupling between a semiconductor laser and a single-mode fiber," *IEEE J. Quantum Electron.*, vol. QE-16, pp. 1067-1072, Oct. 1980.
- [24] D. Gloge, "Dispersion in weakly guiding fibers," *Appl. Opt.*, vol. 10, pp. 2442-2445, Nov. 1971.
- [25] J. Yamada, "Simple dispersion measurement of long-span single-mode fiber using the longitudinal mode spacing of a semiconductor laser," *Opt. Quantum Electron.*, vol. 14, pp. 183-187, Mar. 1982.
- [26] S. Tomaru, M. Yasu, M. Kawachi, and T. Edahiro, "VAD single-mode fiber with 0.2 dB/km loss," *Electron. Lett.*, vol. 17, pp. 92-93, Jan. 1981.

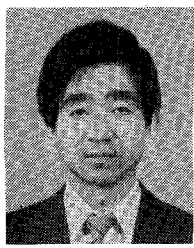
Jun-ichi Yamada, for a photograph and a biography, see p. 573 of the April 1982 issue of this TRANSACTIONS.



Jun-ichi Yamada was born in Tokyo, Japan, on December 7, 1946. He received the B.S. and M.S. degrees from the University of Tokyo, Tokyo, Japan, in 1969 and 1971, respectively.

He joined the Musashino Electrical Communication Laboratory, Nippon Telegraph and Telephone Public Corporation, Tokyo, Japan, in 1971. Since 1974, he has been engaged in research on optical fibers, especially fabrication and characterization of single-mode fibers.

Mr. Yamada is a member of the Institute of Electronics and Communication Engineers of Japan and the Japan Society of Applied Physics.



Tetsuo Miya was born in Niigata, Japan, on February 9, 1950. He received the B.S. and M.S. degrees in physics from the University of Tohoku, Japan, in 1973 and 1975, respectively.

In 1975 he joined the Ibaraki Electrical Communication Laboratory, Nippon Telegraph and Telephone Public Corporation, Ibaraki, Japan, where from 1975 to 1977 he had been engaged in research on the measurement method of refractive index profiles in optical fibers. He is presently a member of the Opto-Materials Device Section, and has been engaged in research on fabrication of single-mode fibers since 1977.

Mr. Miya is a member of the Institute of Electronics and Communication Engineers of Japan.



Haruo Nagai was born in Kanagawa, Japan, in 1943. He received the B.E., M.E., and Ph.D. degrees in applied chemistry from the Keio University, Japan, in 1965, 1967, and 1980, respectively.

In 1967 he joined the Musashino Electrical Communication Laboratory, Nippon Telegraph and Telephone Public Corporation, Tokyo, Japan, where he has been engaged in research on crystal growth for optical device fabrication.

Dr. Nagai is a member of the Japan Society of Applied Physics.

Tatsuya Kimura (S'63-M'68-SM'78), for a photograph and a biography, see p. 65 of the January 1982 issue of the JOURNAL OF QUANTUM ELECTRONICS.

Optical Digital High-Speed Transmission: General Considerations and Experimental Results

WOLFGANG ALBRECHT, CLEMENS BAACK, GERHARD ELZE, BERNHARD ENNING, GÜNTHER HEYDT, LUTZ IHLENBURG, GODEHARD WALF, AND GERHARD WENKE

Abstract—Laboratory experiments on digital optical transmission systems at bit rates of 1 and 2 Gbits/s are described. Systems with graded-index and single-mode fibers in the optical short and long wavelength region were investigated. All systems include complete circuits for clock and signal regeneration. Special emphasis was laid on the development of electronic circuits for gigabit signal processing and on the investigations of the noise sources of the optical channel, which appear especially pronounced in broad-band systems. The experimental results confirm the possibility to set up reliable high-speed optical transmission systems under laboratory conditions with available components. The remaining problems are of optical and not of electronic nature, despite the fact that monolithic integrated circuits for gigabit applications are hardly commercially available today.

I. INTRODUCTION

EXTREMELY rapid progress has been made in the field of optical communications and microelectronics in the last years. This progress allows the engineer to develop future wideband integrated networks, which offer a wide spectrum of narrow- and broad-band services to the subscribers [1], [2].

In cooperation with the German communication industry, an extensive experimental integrated services broad-band communication network was implemented at the Heinrich Hertz Institut (HHI). It consists of optical digital and analog transmission links and applies decentralized as well as centralized

switching. Numerous narrow- and broad-band services, for example, picturephone with color TV qualities, are available [3].

This experimental system contains optical links with nearly all bit rates of the European PCM-hierarchy up to 560 Mbits/s. To investigate optical transmission systems at the higher hierarchy levels of 1.12 and 2.24 Gbits/s a second research project was conducted. The aim was to gain practical experience with such systems and to study the limits of available components as well as the problems which are encountered in the implementation of optical gigabit systems. The results of the work will be illustrated in this paper.

Table I gives a survey of the three systems realized in this project. The first experiments were carried out in the short wavelength region ($\lambda = 0.85 \mu\text{m}$) with graded-index fibers at 1.12 Gbits/s (system 1). It was learned that the graded-index fiber is not suitable for high bit rate transmission. By changing from graded-index fiber to single-mode fiber, a transmission rate of 2.24 Gbits/s was achieved (system 2).

As shown in Fig. 1 the attenuation of the fiber at $0.85 \mu\text{m}$ is about 2 dB/km and the bandwidth of the single-mode fiber is limited by a material dispersion of about $0.1 \text{ ns/km} \cdot \text{nm}$. Lowest attenuation of about 0.5 and 0.2 dB/km is obtained in the long wavelength region (1.3 – $1.6 \mu\text{m}$) [4]. Furthermore, material dispersion disappears at $1.3 \mu\text{m}$; that means at this wavelength the single-mode fiber has an almost unlimited bandwidth. The wavelength of extreme bandwidth can be shifted to $1.55 \mu\text{m}$ by appropriate doping and profile shaping of the fiber core. By this means the wavelength of lowest

Manuscript received March 1, 1982; revised May 19, 1982. This work was supported by the German Bundesministerium für Forschung und Technologie.

The authors are with the Heinrich Hertz Institut für Nachrichtentechnik, Berlin, Germany.